THE JOURNAL OF PHYSICAL CHEMISTRY A

Article

pubs.acs.org/JPCA

Highly Selective Relaxation of the OH Stretching Overtones in Isolated HDO Molecules Observed by Infrared Pump−Repump−Probe Spectroscopy

Daniel Hutzler,[†] Jasper C. Werhahn,[†] Rupert Heider,[†] Maximilian Bradler,[‡] Reinhard Kienberger,*[,†] Eberhard Riedle,[‡] and Hristo Iglev[†]

[†]Physik-Department, Technische Universität München, James-Franck-Strasse, D-85748 Garching, Germany

[‡]Lehrstuhl für BioMolekulare Optik, Ludwig-Maximilians-Universität München, Oettingenstraße 67, D-80538 Munich, Germany

ABSTRACT: A quantitative investigation of the relaxation dynamics of higher-lying vibrational states is afforded by a novel method of infrared pump−repump−probe spectroscopy. The technique is used to study the dynamics of OH stretching overtones in $NaClO_4$·HDO monohydrate. We observe a continuous decrease of the energy separation for the first four states, i.e. ν_{01} = 3575 cm^{-1}, ν_{12} = 3370 cm^{-1}, and ν_{23} = 3170 cm^{-1}, respectively. The population lifetime of the first excited state is 7.2 ps, while the one of the second excited state is largely reduced to 1.4 ps. The relaxation of the v = 2 state proceeds nearly quantitatively to the v = 1 state. The new information on the OH stretching overtones demands improved theoretical potentials and modeling of the H bond interactions. This work shows the potential of the new technique for the precise study of complex vibrational relaxation pathways.

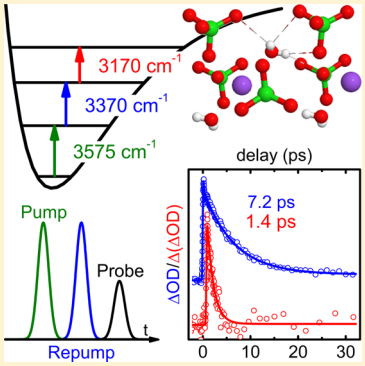

INTRODUCTION

Water is an intriguing substance. Despite being remarkably simple in its chemical composition, the fundamental chemistry that gives rise to its unusual properties is astonishingly poorly understood. Therefore, scientists utilize various techniques to monitor the dynamics and properties of its H bond network on a molecular level and ultrashort time scales.[1,2] Pump−probe infrared (IR) spectroscopy is one of the most prominent tools to access this desired information.[3−7] It is commonly known that stronger H bonds lead to a red-shift of the corresponding OH vibrations and vice versa.[8,9] Thus, the transient response of the OH stretching vibration can be probed to obtain information on the dynamical evolution of the OH group's chemical vicinity. A variety of third-order techniques, i.e. methods described by third order perturbation theory have evolved in this field.[10−18] Typical examples are photon-echo and Kerr effect experiments, which monitor the transient polarization change of the system. In contrast, the pump−probe data measured for delay times longer than the dephasing time, T_2, provide unambiguous information on the population dynamics of the excited state, while the transient phase information is covert. The recently suggested 3D-IR technique,[19,20] a fifth-order experiment, provides overview information on the relaxation dynamics of the first and second excited states.

Pump−repump−probe (PREP) spectroscopy can reach highly excited states by a sequence of pump pulses. Earlier studies demonstrated a comparable technique, where a single moderately broadband IR pump pulse is used for up-pumping the vibrational ladder of the weakly anharmonic CO stretching mode.[21−23] In contrast, the strong anharmonicity of the OH stretching vibration requires the application of independently tunable IR pump, repump, and probe pulses. Using the analogy to time-resolved stimulated 2D Raman spectroscopy,[24−26] PREP can be classified as fifth-order or cascaded pump−probe experiment. The latter denotation is applicable if both pumping processes are spatially (different molecules) or temporally (delay longer than dephasing time) separated from each other.[27,28] PREP has, to this day, mainly focused on UV/vis pump and repump, with varying probe wavelengths.[29−31] These studies demonstrate that a cascade of pump−probe experiments is able to elucidate covert relaxation pathways, while the signal-to-noise ratio of the gained data is comparable to that of standard pump−probe spectroscopy. With our recently developed setup[32] we are now able to perform PREP spectroscopy with ultrashort IR pump, repump, and probe pulses.

Here we present first purely vibrational PREP measurements on the OH stretching mode. The pump pulse excites the OH ν_{01}-transition of quasi-isolated HDO molecules in $NaClO_4$ monohydrate crystals, while the repump is tuned to the first overtone of the OH stretch, ν_{12}. The dynamics of the first and second excited state are recorded with a temporal resolution of sub-200 fs and a spectral accuracy of 5 cm^{-1}. The decay of the 2 → 3 excited state absorption (ESA) and the bleach recovery of the 1 → 2 ESA proceed with the same rate and are both quantitative. This can only be understood as an exclusive

Received: May 29, 2015
Published: June 3, 2015

DOI: 10.1021/acs.jpca.5b05145
J. Phys. Chem. A 2015, 119, 6831−6836

relaxation from the v = 2 to the v = 1 state. The 2 → 1 relaxation proceeds five times faster than the 1 → 0.

EXPERIMENTAL SECTION

The experimental setup used in the time-resolved measurements is described in full detail elsewhere[32] and is just briefly reviewed. The pump and repump pulses are generated by two optical parametric amplifiers with preamplification in the visible.[33] Both systems are pumped by 300 μJ laser pulses at 778 nm with a repetition rate of 1 kHz (provided by CPA-2010; Clark-MXR) and deliver tunable mid-IR pulses with energies of several microjoules. The probe pulses are provided by a single-stage infrared amplifier yielding extremely broadband pulses with spectral widths up to 1 μm at pulse energies of 300 nJ. All three pulses are close to the Fourier limit at pulse durations around 50 fs and therefore deliver a time resolution of sub-100 fs.[32] Since molecular rotations are suppressed in the hydrate crystals, the respective polarizations of all three pulses are identical in this study. In order to avoid spectral overlap between pump and repump pulses and to more precisely pump the OH-stretching transitions in the hydrate a 4*f* spectral selector allows decreasing their spectral bandwidths down to 20 cm^{-1}. Note that a decrease in the bandwidth is accompanied by a decline of the temporal resolution. In the current study the spectrum of the pump pulses was reduced to 90 cm^{-1} yielding a time resolution of sub-200 fs. The time delay of pump and repump pulses with respect to the probe pulse can be set via two independent delay stages. The three pulses are focused onto the sample. To monitor only the central part of the interaction volume with maximum and uniform excitation, the focal size of the probe pulse is 50 μm fwhm and therewith smaller than that of the pump and repump pulses (75 μm fwhm). The probe pulse is coupled into a spectrometer and recorded by a nitrogen cooled 32-channel HgCdTe infrared detector. The spectral resolution of the system is 5 cm^{-1}. Before passing the sample a small part of the probe beam is split off and lead to an additional single channel detector used for normalization in order to reduce shot noise. The energy transmittance of the probe pulse is recorded for four different excitation conditions: $T_{11}(\nu)$ (pump and repump), $T_{10}(\nu)$ (pump only), $T_{01}(\nu)$ (repump only), and $T_{00}(\nu)$ (no excitation). In this way the induced change of the optical density $\Delta OD_{ex}(\nu,t) = -\log(T_{ex}/T_{00})$ is determined for the various excitation conditions (ex = 11, 10, or 01), probe frequencies ν, and delay times. The pump−probe delay is denoted by t_{13}, t_{12} is the pump−repump delay, and t_{23} is the repump−probe delay. The time-resolved data are measured at a sample temperature of 220 K.

The studied sample is derived by crystallization of a saturated solution of $NaClO_4$ dissolved in 15 M HDO in D_2O. The solvent was prepared by isotopic exchange in a mixture of appropriate amounts of D_2O (>99.9 atom % D) and tridistilled H_2O. In the following discussion water always refers to a 15 M HDO/D_2O mixture. The hydrate crystals are grown by slowly cooling a salt solution between two CaF_2 windows in a cryostat at ambient pressure. Steady state IR absorption spectra of the sample were obtained from a commercial VECTOR 22 Fourier-transform infrared spectrometer (FTIR, Bruker Optics) with a spectral resolution of 1 cm^{-1}.

RESULTS AND DISCUSSION

The crystal structure of $NaClO_4$ monohydrate has been determined from X-ray diffraction data.[34] The hydrate forms a monoclinic crystal structure, space group *C*2/*c*, which is schematically illustrated in Figure 1a. The water molecules are

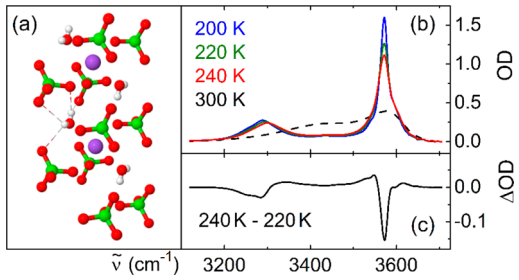

Figure 1. (a) Crystal structure of $NaClO_4$ monohydrate (chlorine atoms green, sodium cations purple, oxygen red, hydrogen white). (b) FTIR absorption spectrum of $NaClO_4$ in $HDO:D_2O$ at different temperatures for the liquid (300 K) and the solid phase. (c) Absorption change for a temperature increase from 220 to 240 K.

bound to the Na cations (purple spheres) with their lone pairs and the OH groups each are bound to two oxygen atoms of neighboring ClO_4 anions by very weak, bifurcated H bonds. The closest distance between two water molecules is 440 pm, they are distinctly separated from each other through the perchlorate anions. Note that in the used isotopic mixture, on average only every fourth water molecule contains an OH group, which leads to an even larger separation of the OH oscillators. Therefore, this hydrate system delivers the possibility to investigate the characteristic dynamics of quasi-isolated HDO monomers.

Figure 1b shows the FTIR spectra of the $NaClO_4$·HDO sample at various temperatures. The low solubility of $NaClO_4$ leads to formation of a polycrystalline hydrate−ice sample upon cooling. The weak interaction between water molecules and the perchlorate anions has been noted before[35] and gives rise to the feature at 3575 cm^{-1}, which is blue-shifted in comparison to the well-known ice peak at 3295 cm^{-1}. The well-defined spatial separation of ice and hydrate phase can be deduced from the additivity of both spectral features, in an analogous fashion to the analysis presented in ref 36. The spectral width of the hydrate peak is 36 cm^{-1} and that of the ice band 107 cm^{-1}. Figure 1b shows a significant rise of the amplitude of the hydrate peak for lower temperatures, while the ice band shows a lower amplitude increase accompanied by an almost linear spectral shift of the peak maximum.[37] The thermal differential spectrum for a temperature jump from 220 to 240 K, shown in Figure 1c, indicates two conspicuous features due to heating of the ice and the hydrate phase, respectively.

The pump−probe data, $\Delta OD(\nu,t_{13}) = -\log(T_{10}/T_{00})$, measured after excitation in the maximum of the OH stretching band of the $NaClO_4$ monohydrate and blocked repump are presented in Figure 2a−d. The transient spectra show that the optical excitation leads to a ground state bleaching (GSB) at 3575 cm^{-1} and a 1 → 2 excited state absorption (ESA_{12}) that is spectrally shifted to 3370 cm^{-1} due to the anharmonicity of the OH stretching mode (Figures 2a and b). The spectral width of the ESA_{12} (50 cm^{-1} fwhm) is significantly larger than that of the GSB (40 cm^{-1}). The extracted population lifetime of the first excited state v = 1 (see below) indicates that the spectral width of the 0 → 1 transition is dominated by dephasing, which

DOI: 10.1021/acs.jpca.5b05145
J. Phys. Chem. A 2015, 119, 6831−6836

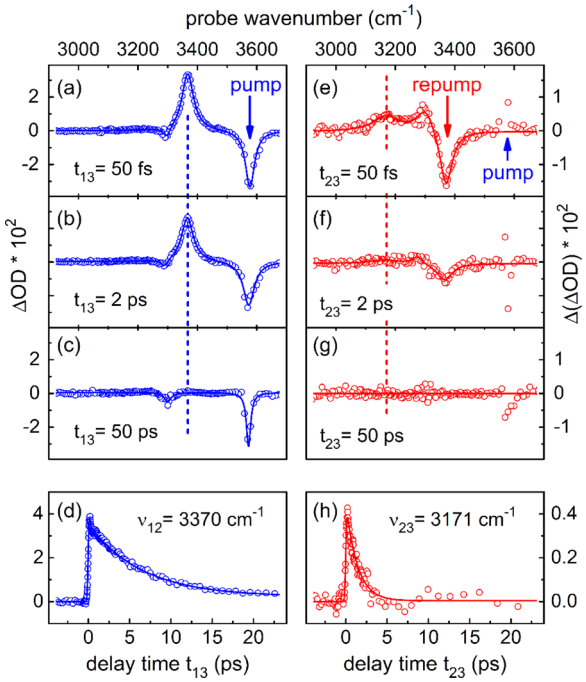

Figure 2. (a–c) Pump–probe spectra after excitation of the hydrate peak at ν_{01} = 3575 cm^{-1} for three different pump–probe delays t_{13}. The data show a bleaching of the ν_{01}-transition and an excited state absorption at ν_{12}. (d) Transient measured at ν_{12} = 3370 cm^{-1}. (e–g) Transient PREP spectra after pumping at ν_{01} and repumping at ν_{12}. The pump–repump delay t_{12} is fixed at 750 fs, and the repump–probe delay time t_{23} is varied. (h) PREP signal in the maximum of the repump-induced second ESA at ν_{23} = 3170 cm^{-1}. Measured data are shown as circlets and fits as solid lines.

is most probably due to coupling with low-frequency librational modes. This coupling seems to be stronger for the OH overtones. The small feature at 3295 cm^{-1} can be ascribed to the spatially separated ice crystal structure in the sample that has been discussed above.

The absorption changes measured at 50 ps (see Figure 2c) are assigned to a laser-induced transient heating of the sample. The qualitative agreement of the data with the thermal differential spectrum shown in Figure 1c supports this assumption; however, the smaller amplitude of the transient data in Figure 2c indicates a much smaller temperature jump of about 4 K. Furthermore, the laser-induced heating occurs at almost constant volume resulting in a simultaneous pressure increase,[37,38] leading to the small difference in the shape of the thermal differential spectra measured in FTIR and pump–probe data. We emphasize that the laser-induced heating recovers in the time window between two pump pulses,[38] so no measurable long-time heating of the sample is observed.

The relaxation dynamics of the quasi-isolated OH vibration is illustrated in Figure 2d, where the temporal evolution of the absorption changes measured at the maximum of the ESA_{12} is plotted. The process is dominated by a monoexponential decay with a time constant of 7.2 ± 0.5 ps. The rapid signal change observed within the first 200 fs is treated as coherent artifact[32] and will not be further discussed. According to Fermi's Golden Rule the relaxation time depends on the existence of appropriate accepting modes and their coupling strengths to the initially excited OH vibration. Our earlier studies on NaCl·2HDO and $LiNO_3$·3HDO hydrates support this conclusion.[36,39] The perchlorate anions supply the ClO stretching vibration with a frequency of 1100 cm^{-1} that in combination with the OD stretching mode (at roughly 2400 cm^{-1}) could be effectively accessed as a relaxation channel for the OH stretching. However, the weak coupling of the HDO molecule to the environment strongly hinders this relaxation process. Studies on isotopically dilute water pointed the important role of the bending overtone (δ = 2, at roughly 2925 cm^{-1} for HDO) for relaxation of the OH stretching mode.[40−42] The larger energy mismatch between v,δ = 1,0 and 0,2 mode and the weaker coupling of the water molecules in $NaClO_4$ monohydrate leads to a relaxation rate, which is an order of magnitude smaller than that measured in HDO:D_2O water and ice.[43] Our conclusions are in accordance with the results of Bakker et al. for HDO monomers bound to acetone in the liquid phase, where the OH vibration at 3530 cm^{-1} shows a lifetime of 6.3 ± 0.3 ps.[44]

The properties of higher overtones of the OH stretching vibration are studied using pump–repump–probe (PREP) spectroscopy. Here the pump pulse is resonant with ν_{01}, while the repump pulse is centered at the ν_{12} transition. The peak intensities of both pulses are in the range of 250 GW/cm^2 and therefore high enough to generate a measurable population of the v = 2 overtone of the OH stretching vibration. The probe pulse covers a broad spectral range in the mid-IR, but of particular interest will be the data at the spectral positions of the first and second excited state absorption, ESA_{12} and ESA_{23}.

The probe absorption changes measured 800 fs after excitation at ν_{01} = 3575 cm^{-1} and secondary excitation 750 fs after the pump pulse (i.e., repump at ν_{12} = 3370 cm^{-1} and t_{23} = 50 fs) are shown in green in Figure 3a. The simultaneously measured pump–probe signal (repump blocked) is shown in blue for comparison. Note that an excitation of the sample by the repump without a prior excitation by the pump induces no significant effect in the hydrate. However, the weak absorption of the ice fraction at the repump frequency leads to a small transient heating of the sample. To compensate for this signal, the pump–repump–probe data (green circlets in Figure 3a) are calculated by comparison of the probe transmission after two pulse excitation to the probe transmission after excitation with the repump only, i.e. $\Delta OD_{PuRe}(\nu,t) = -\log(T_{11}/T_{01})$.

Both spectra in Figure 3a show the ground state bleaching at ν_{01} and the first excited state absorption (ESA_{12}) at ν_{12}. The difference between green and blue data

$$\Delta(\Delta OD) = -\log\left(\left(\frac{T_{11}}{T_{00}} - \log\frac{T_{01}}{T_{00}}\right) - \log\frac{T_{10}}{T_{00}}\right) = -\log\left(\frac{T_{11}\cdot T_{00}}{T_{01}\cdot T_{10}}\right) \quad (1)$$

is the PREP signal (Figure 3b). Similar data processing was applied in earlier three-pulse spectroscopic studies.[30] Two main features are observable: a bleaching of the ESA_{12} and a second excited state absorption (ESA_{23}) at ν_{23} = 3170 cm^{-1} (see also Figure 2e–g). Note that pre-excitation by the pump induces a pressure and temperature jump and therefore modifies the ice and hydrate absorption bands. This effect leads to an overestimation of the probe absorption changes measured after excitation with the repump only. This is manifested by an additional absorption at 3295 cm^{-1}, i.e. around the steady state absorption of the ice fraction and a stray signal around 3575 cm^{-1}. Moreover, the lower sample transmission in the

DOI: 10.1021/acs.jpca.5b05145
J. Phys. Chem. A 2015, 119, 6831−6836

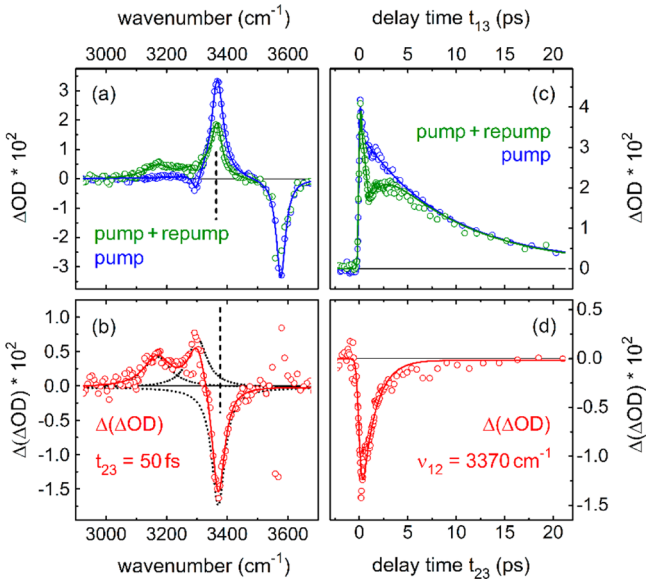

Figure 3. Principle of vibrational PREP spectroscopy. (a) Probe absorption changes measured after pumping at ν_{01} and repumping at ν_{12} in green. The pump−repump delay time t_{12} is 750 fs, while the repump−probe delay time t_{23} is 50 fs. The according pump−probe signal is given in blue for comparison. (b) Difference signal $\Delta(\Delta\mathrm{OD})$ between the 3- and 2-pulse data shown in part a. The bleaching at ν_{12} = 3370 cm^{-1}, the absorption of the second excited state at ν_{23} = 3170 cm^{-1}, and the contribution of the ice fraction at 3295 cm^{-1} are indicated by dashed lines. (c) Absorption changes measured at ν_{12} as in a (green). The corresponding pump−probe signal is shown in blue. (d) Difference between both curves in part c representing the transient evolution of the repump-induced bleaching of the first excited state. The extracted time constant is the same as in Figure 2h.

maximum of ice and hydrate bands reduces the signal-to-noise ratio of the transient signals at these frequencies.

The data in Figure 3b are analyzed by Lorentzian distributions (dashed lines) and the red solid line displays the resulting cumulative fit. The extracted spectral width of ESA_{23} of 105 ± 30 cm^{-1} is a factor of 2 larger than that of the ESA_{12}. This indicates further increase of the coupling to the environment in agreement with 3D-IR studies on ice.[20] The transient PREP spectra measured for different delay times t_{23} (see Figures 2e−g) show that the signals due to absorption of the first two OH-stretching overtones decay completely within the first 10 ps.

Our pump−probe and PREP measurements reveal energy gaps of ν_{01} = 3575 cm^{-1}, ν_{12} = 3370 cm^{-1}, and ν_{23} = 3170 cm^{-1} for the first three vibrational transitions. Obviously, the distance between adjacent energy states decreases for higher quantum numbers, while the frequency shift seems to remain constant or even to be slightly reduced for higher states ($\nu_{01} - \nu_{12}$ = 205 cm^{-1}, while $\nu_{12} - \nu_{23}$ = 200 cm^{-1}). The energy shift describing the shrinking of the gaps between neighboring states can be regarded as a quantitative expression for the anharmonicity of the OH potential. Various analytic functions have been applied for modeling the OH potential's energy surface.[45,46] Particularly, the Lippincott−Schroeder (LS) potential has been used before to simulate IR pump−probe and 2D-IR spectra of water[47,48] and aqueous hydrates.[49] Generally, the potential describing the H bonds in aqueous hydrates includes three terms representing the intramolecular and intermolecular interaction of the proton and the interaction of the oxygen with the surrounding. For OH groups engaged in weak H-bonds, as the one studied here, the potential is dominated by the first term: $V^{LS}(r_{OH}) = D_e^{LS}(1 - \exp\{-n(r_{OH} - r_0)^2/2r_{OH}\})$. Here D_e^{LS} denotes the potential depth, r_0 is the O−H separation at equilibrium position, and n is the potential factor. The typical values for the latter are between 9.15 and 10.2 $Å^{-1}$ (on average 9.55 $Å^{-1}$), while the OH equilibrium separation is about r_0 = 0.97 Å.[20,47,49] Applying these numbers to the LS potential and solving the Schrödinger equation delivers OH frequencies of ν_{01} = 3574 cm^{-1}, ν_{12} = 3369 cm^{-1}, and ν_{23} = 3158 cm^{-1}. These results, gained for a reduced mass of $\mu = 1.225 \times 10^{-27}$ kg and D_e^{LS} = 29800 cm^{-1}, are in very good agreement with the experimental data.

On the other hand, the almost constant frequency downshift with an average energy of 202.5 cm^{-1} measured for ν_{01}, ν_{12}, and ν_{23} suggests a potential that features constant anharmonicity, such as Morse: $V^{M}(r_{OH}) = D_e^{M}(1 - \exp\{-a(r_{OH} - r_0)\})^2$ with the potential factor a. Since the Schrödinger equation can be solved analytically for Morse potentials, the extracted potential depth is D_e^{M} = 35250 cm^{-1}, which is close to the O−H binding energy of water of 38750 cm^{-1}.[47] Using our results for D_e^{M} and the reduced mass, estimated for the LS potential, yields a potential factor of a = 2.8 $Å^{-1}$. We emphasize that our simple estimations do not verify the optimal OH potential but rather demonstrate that the new information on the OH stretching overtones can help to improve theoretical potentials and to model the H bond interactions.

Figure 3c shows the probe absorption changes measured at ν_{12} = 3370 cm^{-1} for pumping at ν_{01} and repumping at ν_{12} and fixed t_{12} = 750 fs, for various pump−probe delay times t_{13} (green). The corresponding pump−probe transient is depicted in blue. It can immediately be seen that the repumping bleaches the ESA_{12}. The repump-induced signal decrease fully recovers within 10 ps so that the 2- and 3-pulse data coincide almost perfectly for probe delays longer than 10 ps. The PREP signal transient shown in Figure 3d is the difference $\Delta(\Delta\mathrm{OD})$ between both data sets and illustrates the temporal evolution of the first excited state bleaching. Figure 2h shows the dynamics of the ESA_{23} measured at 3170 cm^{-1} under the same excitation conditions. The ESA_{23} decays exponentially with a time constant of 1.4 ± 0.2 ps which is the population lifetime of the v = 2 state. Regarding the two lifetimes of first (7.2 ps) and second excited state (1.4 ps) we recognize a rather large reduction by a factor of 5.2. The better overlap of the wave functions for the 1 → 2 transition compared to 0 → 1 would suggest a corresponding lifetime shortening by a factor of only 2, which has been experimentally verified in an earlier study on the CO stretching vibration in gas phase.[21] Possible reasons for a larger factor in $NaClO_4$ monohydrate are a more efficient energy transfer to high-lying combination tones or the invoking of nonadiabatic vibrational relaxation to v = 1 as observed in ice.[20]

The bleach of the ESA_{12} recovers with the same time constant as the ESA_{23} decays. The equality of these two times is quantitative evidence that the second excited state decays virtually exclusively to the first excited state. This is also corroborated by the fact that the PREP signal in Figure 3d returns to zero within experimental accuracy. This observation gives evidence that the OH stretching overtone relaxes to a combination tone of the OH stretch with other modes, most probably the bending overtone (v,δ = 1,2).[40−42] Due to the smaller energy mismatch between v,δ = 2,0 and 1,2 than between 1,0 and 0,2, this assumption also could explain the

DOI: 10.1021/acs.jpca.5b05145
J. Phys. Chem. A 2015, 119, 6831−6836

significantly shorter lifetime of the OH stretching overtone, discussed just above.

CONCLUSION

In conclusion, we have presented the first pump−repump−probe measurements with exclusively mid-IR pulses, to study the properties and relaxation pathways of higher-lying OH vibrational states. Our data show that vibrational PREP is not only capable of yielding quantitative lifetimes and spectral positions of higher-lying vibrational states, but can also unravel the relaxation pathway of high-lying vibrations. Both the relaxation rate and relaxation path can be determined from experimental data without any complex modeling. As the time delay is rapidly scanned, the decay dynamics can be determined with high precision, while in multidimensional spectroscopies a tedious sequence of spectrograms has to be recorded. It should be noted that the analysis of PREP data measured in complex H-bonded systems as ice and liquid water can be more complicated than in $NaClO_4$ monohydrate; nevertheless, our earlier experiments on electron photodetachment already demonstrated the ability of PREP spectroscopy to map covert relaxation mechanisms.[27,31] An obvious application of our research is the obtainment of the necessary parameters for a theoretical model capable of a profound and precise description of the H bond interaction. With our experimental data we are able to scan the shape of the OH potential to high-lying energetic regions and provide this new information as additional input parameters to theoretical calculations and simulations. We have also demonstrated, that the frequency resolved probe measurements can help untangle the oftentimes complex relaxation pathways of high-lying vibrational states.

AUTHOR INFORMATION

Corresponding Author

*E-mail: reinhard.kienberger@tum.de.

Notes

The authors declare no competing financial interest.

ACKNOWLEDGMENTS

The authors thank K. Beltinger for her support in the data analysis. Financial support of this work by Deutsche Forschungsgemeinschaft through the excellence cluster "Munich Center for Advanced Photonics" (MAP) is gratefully acknowledged.

REFERENCES

(1) Nibbering, E. T.; Elsaesser, T. Ultrafast vibrational dynamics of hydrogen bonds in the condensed phase. *Chem. Rev.* **2004**, *104* (4), 1887−1914.
(2) Bakker, H.; Skinner, J. Vibrational spectroscopy as a probe of structure and dynamics in liquid water. *Chem. Rev.* **2010**, *110* (3), 1498−1517.
(3) Graener, H.; Seifert, G.; Laubereau, A. New spectroscopy of water using tunable picosecond pulses in the infrared. *Phys. Rev. Lett.* **1991**, *66* (16), 2092.
(4) Laenen, R.; Rauscher, C.; Laubereau, A. Dynamics of local substructures in water observed by ultrafast infrared hole burning. *Phys. Rev. Lett.* **1998**, *80* (12), 2622.
(5) Woutersen, S.; Emmerichs, U.; Bakker, H. Femtosecond mid-IR pump-probe spectroscopy of liquid water: Evidence for a two-component structure. *Science* **1997**, *278* (5338), 658−660.
(6) Gale, G.; Gallot, G.; Hache, F.; Lascoux, N.; Bratos, S.; Leicknam, J.-C. Femtosecond dynamics of hydrogen bonds in liquid water: A real time study. *Phys. Rev. Lett.* **1999**, *82* (5), 1068.
(7) Lindner, J.; Vöhringer, P.; Pshenichnikov, M. S.; Cringus, D.; Wiersma, D. A.; Mostovoy, M. Vibrational relaxation of pure liquid water. *Chem. Phys. Lett.* **2006**, *421* (4), 329−333.
(8) Eisenberg, D.; Kauzmann, W. *The structure and properties of water*; Clarendon: Oxford, 1969.
(9) Franks, F. *Water: A comprehensive treatise*; Plenum Press, 1972
(10) Torre, R.; Bartolini, P.; Righini, R. Structural relaxation in supercooled water by time-resolved spectroscopy. *Nature* **2004**, *428* (6980), 296−299.
(11) Sovago, M.; Campen, R. K.; Wurpel, G. W.; Müller, M.; Bakker, H. J.; Bonn, M. Vibrational response of hydrogen-bonded interfacial water is dominated by intramolecular coupling. *Phys. Rev. Lett.* **2008**, *100* (17), 173901.
(12) Stenger, J.; Madsen, D.; Hamm, P.; Nibbering, E. T.; Elsaesser, T. Ultrafast vibrational dephasing of liquid water. *Phys. Rev. Lett.* **2001**, *87* (2), 027401.
(13) Golonzka, O.; Khalil, M.; Demirdöven, N.; Tokmakoff, A. Vibrational anharmonicities revealed by coherent two-dimensional infrared spectroscopy. *Phys. Rev. Lett.* **2001**, *86* (10), 2154.
(14) Savolainen, J.; Ahmed, S.; Hamm, P. Two-dimensional raman-terahertz spectroscopy of water. *Proc. Natl. Acad. Sci. U. S. A.* **2013**, *110* (51), 20402−20407.
(15) Fecko, C.; Eaves, J.; Loparo, J.; Tokmakoff, A.; Geissler, P. Ultrafast hydrogen-bond dynamics in the infrared spectroscopy of water. *Science* **2003**, *301* (5640), 1698−1702.
(16) Cowan, M.; Bruner, B. D.; Huse, N.; Dwyer, J.; Chugh, B.; Nibbering, E.; Elsaesser, T.; Miller, R. Ultrafast memory loss and energy redistribution in the hydrogen bond network of liquid H2O. *Nature* **2005**, *434* (7030), 199−202.
(17) Asbury, J. B.; Steinel, T.; Kwak, K.; Corcelli, S.; Lawrence, C.; Skinner, J.; Fayer, M. Dynamics of water probed with vibrational echo correlation spectroscopy. *J. Chem. Phys.* **2004**, *121* (24), 12431−12446.
(18) Park, S.; Kwak, K.; Fayer, M. Ultrafast 2D-IR vibrational echo spectroscopy: a probe of molecular dynamics. *Laser Phys. Lett.* **2007**, *4* (10), 704.
(19) Garrett-Roe, S.; Perakis, F.; Rao, F.; Hamm, P. Three-dimensional infrared spectroscopy of isotope-substituted liquid water reveals heterogeneous dynamics. *J. Phys. Chem. B* **2011**, *115* (21), 6976−6984.
(20) Perakis, F.; Borek, J. A.; Hamm, P. Three-dimensional infrared spectroscopy of isotope-diluted ice Ih. *J. Chem. Phys.* **2013**, *139* (1), 014501.
(21) Arrivo, S. M.; Dougherty, T. P.; Grubbs, W. T.; Heilweil, E. J. Ultrafast infrared spectroscopy of vibrational CO-stretch up-pumping and relaxation dynamics of W (CO)< sub> 6</sub>. *Chem. Phys. Lett.* **1995**, *235* (3), 247−254.
(22) Witte, T.; Yeston, J.; Motzkus, M.; Heilweil, E.; Kompa, K.-L. Femtosecond infrared coherent excitation of liquid phase vibrational population distributions (v>5). *Chem. Phys. Lett.* **2004**, *392* (1), 156−161.
(23) Disselkamp, R.; Ewing, G. E. High vibrational states of carbon monoxide in liquid argon: overtone intensity enhancement and reactions with oxygen. *J. Phys. Chem.* **1989**, *93* (17), 6334−6339.
(24) Blank, D. A.; Kaufman, L. J.; Fleming, G. R. Fifth-order two-dimensional Raman spectra of CS2 are dominated by third-order cascades. *J. Chem. Phys.* **1999**, *111* (7), 3105−3114.
(25) Ulness, D. J.; Kirkwood, J. C.; Albrecht, A. Competitive events in fifth order time resolved coherent Raman scattering: Direct versus sequential processes. *J. Chem. Phys.* **1998**, *108* (10), 3897−3902.
(26) Zhao, B.; Sun, Z.; Lee, S.-Y. Quantum theory of time-resolved femtosecond stimulated Raman spectroscopy: Direct versus cascade processes and application to CDCl3. *J. Chem. Phys.* **2011**, *134* (2), 024307.
(27) Fischer, M. K.; Laubereau, A.; Iglev, H. Femtosecond electron detachment of aqueous bromide studied by two and three pulse spectroscopy. *Phys. Chem. Chem. Phys.* **2009**, *11* (46), 10939−10944.
(28) Wilson, K. C.; Lyons, B.; Mehlenbacher, R.; Sabatini, R.; McCamant, D. W. Two-dimensional femtosecond stimulated Raman

DOI: 10.1021/acs.jpca.5b05145
J. Phys. Chem. A 2015, 119, 6831−6836

spectroscopy: observation of cascading Raman signals in acetonitrile. *J. Chem. Phys.* **2009**, *131* (21), 214502.
(29) Martini, I. B.; Barthel, E. R.; Schwartz, B. J. Optical control of electrons during electron transfer. *Science* **2001**, *293* (5529), 462−465.
(30) Buback, J.; Kullmann, M.; Langhojer, F.; Nuernberger, P.; Schmidt, R.; Wurthner, F.; Brixner, T. Ultrafast bidirectional photoswitching of a spiropyran. *J. Am. Chem. Soc.* **2010**, *132* (46), 16510−16519.
(31) Iglev, H.; Fischer, M. K.; Gliserin, A.; Laubereau, A. Ultrafast geminate recombination after photodetachment of aqueous hydroxide. *J. Am. Chem. Soc.* **2011**, *133* (4), 790−795.
(32) Bradler, M.; Werhahn, J. C.; Hutzler, D.; Fuhrmann, S.; Heider, R.; Riedle, E.; Iglev, H.; Kienberger, R. A novel setup for femtosecond pump-repump-probe IR spectroscopy with few cycle CEP stable pulses. *Opt. Express* **2013**, *21* (17), 20145−20158.
(33) Bradler, M.; Homann, C.; Riedle, E. Mid-IR femtosecond pulse generation on the microjoule level up to 5 μm at high repetition rates. *Opt. Lett.* **2011**, *36* (21), 4212−4214.
(34) Berglund, B.; Thomas, J. O.; Tellgren, R. Hydrogen bond studies. CII. An X-ray determination of the crystal structure of sodium perchlorate monohydrate, NaClO4. H2O. *Acta Crystallogr., Sect. B: Struct. Crystallogr. Cryst. Chem.* **1975**, *31* (7), 1842−1846.
(35) Walrafen, G. Raman spectral studies of the effects of perchlorate ion on water structure. *J. Chem. Phys.* **1970**, *52* (8), 4176−4198.
(36) Pandelov, S.; Pilles, B. M.; Werhahn, J. C.; Iglev, H. Time-resolved dynamics of the OH stretching vibration in aqueous NaCl hydrate. *J. Phys. Chem. A* **2009**, *113* (38), 10184−10188.
(37) Iglev, H.; Schmeisser, M.; Simeonidis, K.; Thaller, A.; Laubereau, A. Ultrafast superheating and melting of bulk ice. *Nature* **2006**, *439* (7073), 183−186.
(38) Schmeisser, M.; Iglev, H.; Laubereau, A. Maximum superheating of bulk ice. *Chem. Phys. Lett.* **2007**, *442* (4), 171−175.
(39) Werhahn, J. C.; Pandelov, S.; Xantheas, S. S.; Iglev, H. Dynamics of weak, bifurcated, and strong hydrogen bonds in lithium nitrate trihydrate. *J. Phys. Chem. Lett.* **2011**, *2* (13), 1633−1638.
(40) Lawrence, C. P.; Skinner, J. L. Vibrational spectroscopy of HOD in liquid D2O. I. Vibrational energy relaxation. *J. Chem. Phys.* **2002**, *117* (12), 5827−5838.
(41) Rey, R.; Møller, K. B.; Hynes, J. T. Ultrafast vibrational population dynamics of water and related systems: A theoretical perspective. *Chem. Rev.* **2004**, *104* (4), 1915−1928.
(42) De Marco, L.; Ramasesha, K.; Tokmakoff, A. Experimental evidence of Fermi resonances in isotopically dilute water from ultrafast broadband IR spectroscopy. *J. Phys. Chem. B* **2013**, *117* (49), 15319−15327.
(43) Woutersen, S.; Emmerichs, U.; Nienhuys, H.-K.; Bakker, H. J. Anomalous temperature dependence of vibrational lifetimes in water and ice. *Phys. Rev. Lett.* **1998**, *81* (5), 1106.
(44) Bakker, H. J.; Gilijamse, J. J.; Lock, A. J. Energy Transfer in Single Hydrogen-Bonded Water Molecules. *ChemPhysChem* **2005**, *6* (6), 1146−1156.
(45) Xantheas, S. S.; Werhahn, J. C. Universal scaling of potential energy functions describing intermolecular interactions. I. Foundations and scalable forms of new generalized Mie, Lennard-Jones, Morse, and Buckingham exponential-6 potentials. *J. Chem. Phys.* **2014**, *141* (6), 064117.
(46) Werhahn, J. C.; Akase, D.; Xantheas, S. S. Universal scaling of potential energy functions describing intermolecular interactions. II. The halide-water and alkali metal-water interactions. *J. Chem. Phys.* **2014**, *141* (6), 064118.
(47) Bakker, H.; Nienhuys, H.-K. Delocalization of protons in liquid water. *Science* **2002**, *297* (5581), 587−590.
(48) Perakis, F.; Hamm, P. 2D IR Spectroscopy of Ice Ih. *International Conference on Ultrafast Structural Dynamics*, Berlin, March 19−21; Optical Society of America, 2012; p IW3D.5.
(49) Kim, H.-J.; Yoon, B.-G. Study of the Librational Motion of H_2O Molecules in Hydrates by Neutron Inelastic Scattering. *J. Korean Nucl. Soc.* **1979**, *11* (1), 1−20.

DOI: 10.1021/acs.jpca.5b05145
J. Phys. Chem. A 2015, 119, 6831−6836